Langmuir

Article

pubs.acs.org/Langmuir

Controllable Hierarchical Microstructures Self-Assembled from Multiblock Copolymers Confined in Thin Films

Xu Zhang, Liquan Wang,* Liangshun Zhang, Jiaping Lin,* and Tao Jiang

Shanghai Key Laboratory of Advanced Polymeric Materials, State Key Laboratory of Bioreactor Engineering, Key Laboratory for Ultrafine Materials of Ministry of Education, School of Materials Science and Engineering, East China University of Science and Technology, Shanghai 200237, China

Supporting Information

ABSTRACT: Hierarchical microstructures self-assembled from $A(BC)_n$ multiblock copolymers confined between two solid surfaces were explored by dissipative particle dynamics simulations. The strategy using confinement allows us to generate hierarchical microstructures with various numbers and different orientations of small-length-scale lamellae. Except for the hierarchical lamellar microstructures with parallel or perpendicular arrangements of small-length-scale lamellae, the coexistence of two different hierarchical lamellae was also discovered by varying the film thickness. The dynamics of hierarchical microstructure formation was further examined. It was found that the formation of the hierarchical microstructures exhibits a stepwise manner where the formation of small-length-scale structures lags behind that of large-length-scale structures. The present work could provide guidance for controllable manufacture of hierarchical microstructures.

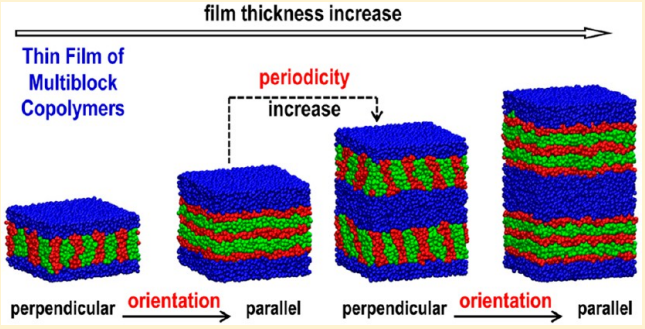

1. INTRODUCTION

The hierarchical characteristic of materials, which appears in collagen, abalone nacre, and dendrons, is ubiquitous in nature.[1−5] This natural phenomenon has stimulated researchers to fabricate synthetic materials presenting complex hierarchical microstructures. These materials have promising applications in smart coatings, biosensors, and fuel cells.[6] Benefited in the latent applications of materials with hierarchical microstructures, the field of hierarchical microstructures has undergone rapid growth over the last decades. Block copolymers, an important class of soft matter, are capable of self-assembling into hierarchical microstructures.[7−9] The possibility of forming hierarchical microstructures from block copolymers could bring a significant advance in applications requiring materials with multiple-length-scale microstructures.

Recent efforts have greatly contributed to creating hierarchical microstructures with double length scales by virtue of the self-assembly of precisely building molecules such as $A(BC)_n$ and $A(BC)_nBA$ multiblock copolymers consisting of one or two tails and many midblocks. These types of multiblock copolymers can self-assemble into parallel and perpendicular packed hierarchical microstructures with two different length scales.[10−13] The orientation and number of small-length-scale lamellae can be tailored by tuning the parameters such as the number of the midblocks and the interaction strength.[13] Despite the advances in creating microstructures with multiple length scales, it is still far from understanding the nature of hierarchies and meeting the demands in practical applications because diversified molecules should be synthesized to generate the desired microstructures. Thus, questions arise as to whether we can obtain the required hierarchical microstructures with a different orientation or various numbers of small-length-scale lamellae simultaneously from one specific multiblock copolymer system. Using solid surfaces to direct the self-assembly of multiblock copolymers in thin films could be an effective way to obtain desired structures.[14−25]

The thin films of block copolymers have been extensively studied for their potential applications in fields of surface coating, nanomembrane, and nanolithography.[26,27] It was well documented that, for the lamellar microstructures self-assembled from diblock copolymers in confinement, the number of the layers and the orientation of the layers to the solid surfaces can be tuned by the film thickness.[14,21,28−34] Likewise, directed self-assembly of multiblock copolymers in thin films could, in principle, create hierarchical lamellae with various numbers and orientations of small-length-scale lamellae. To date, there are rare studies concerning the self-assembly of multiblock copolymers in thin films, and therefore, how the confinement influences the hierarchical microstructures still remains unknown. In addition, insight into the dynamics of hierarchical microstructure formation is also an important issue which has not been well addressed yet due to the complexity of the multiblock copolymer systems. As far as we know, less

Received: October 7, 2014
Revised: January 30, 2015
Published: February 5, 2015

DOI: 10.1021/la503985u
Langmuir 2015, 31, 2533−2544

attention has been paid to the dynamics of the microphase separation of block copolymer in thin films.

Theories and simulations have emerged as powerful tools for studying self-assembly behaviors of complex copolymer systems.[35−38] One of the useful approaches is the dissipative particle dynamics (DPD) method. The DPD method, originally proposed by Hoogerbrugge and Koelman,[39,40] is a particle-based mesoscopic simulation technique particularly suitable for complex fluids. It has been effectively employed to understand the self-assembly behaviors of forming hierarchical microstructures.[11,41] ten Brinke and co-workers have observed hierarchical lamellae-in-lamellar microstructures with three, five, or seven internal layers in the small-length-scale structures self-assembled from ternary $A(BC)_nBA$ multiblock copolymers by DPD simulation.[11] Moreover, it has also been used to study the phase behaviors of confined block copolymers. Liu et al. have investigated the morphologies of diblock copolymers confined in a cylindrical tube by DPD.[42] It was found that, when the tube wall is nonuniform toward the two blocks, as the diameter of the tube increases, perpendicular lamellae change first to parallel lamellae and then back to perpendicular lamellae. These results suggest that the DPD method can well be applied to study the hierarchical microstructures formed in confined thin films of multiblock copolymers.

In this work, we employed the laterally parallel confinement technique to direct the self-assembly of multiblock copolymers with the architecture of $A(BC)_n$ style to self-assemble into various controlled hierarchical microstructures. The DPD method was employed for this study. The effects of the film thickness and the interaction strength on the hierarchical microstructures were examined. It was found that the hierarchical microstructures exhibit not only a transition from parallel to perpendicular hierarchical lamellae but also a variation of the number of the small-length-scale lamellae. In addition, the dynamics of hierarchical microstructure formation was further studied.

2. SIMULATION METHOD

2.1. Dissipative Particle Dynamics. Dissipative particle dynamics (DPD) is a combination of molecular dynamics, lattice-gas automata, and Langevin dynamics. It obeys Galilean invariance, isotropy, mass conservation, and momentum conservation. In the DPD simulation, a particle with mass m represents a block or cluster of atoms or molecules moving together in a coherent fashion. These DPD particles are subject to soft potentials and governed by predefined collision rules.[43] The time evolution of the particle system can be found by solving Newton's equations of motion

$$\frac{d\mathbf{r}_\alpha}{dt} = \mathbf{v}_\alpha, \qquad m_\alpha \frac{d\mathbf{v}_\alpha}{dt} = \mathbf{f}_\alpha \tag{1}$$

where m_α, $\mathbf{r}_\alpha$, $\mathbf{v}_\alpha$, and $\mathbf{f}_\alpha$ denote the mass, position, and velocity of the αth particle and the force acting on it, respectively. For simplicity, the masses of the particles are set to be unity.

The time integration of motion equations is done by a modified velocity-Verlet algorithm[44,45]

$$\begin{aligned}
\mathbf{r}_\alpha(t+\Delta t) &= \mathbf{r}_\alpha(t) + \Delta t\mathbf{v}_\alpha(t) + 0.5(\Delta t)^2\mathbf{f}_\alpha(t)\\
\tilde{\mathbf{v}}_\alpha(t+\Delta t) &= \mathbf{v}_\alpha(t) + \lambda\Delta t\mathbf{f}_\alpha(t)\\
\mathbf{f}_\alpha(t+\Delta t) &= \mathbf{f}_\alpha(\mathbf{r}(t+\Delta t), \tilde{\mathbf{v}}(t+\Delta t))\\
\mathbf{v}_\alpha(t+\Delta t) &= \mathbf{v}_\alpha(t) + 0.5\Delta t(\mathbf{f}_\alpha(t) + \mathbf{f}_\alpha(t+\Delta t))
\end{aligned} \tag{2}$$

where $\tilde{\mathbf{v}}_\alpha(t+\Delta t)$ and $\mathbf{v}_\alpha(t+\Delta t)$ denote the erroneous and modified velocities at $t+\Delta t$. According to the work of Groot and Warren,[44] we chose $\lambda = 0.65$ and $\Delta t = 0.04\tau$ (τ is time unit).

In the method, the nonbonded force acting on a particle, $\mathbf{f}_\alpha$, is a pairwise additive force, consisting of the conservative force ($\mathbf{F}^C_{\alpha\beta}$), dissipative force ($\mathbf{F}^D_{\alpha\beta}$), and random force ($\mathbf{F}^R_{\alpha\beta}$)[44]

$$\mathbf{f}_\alpha = \sum_{\beta\neq\alpha} (\mathbf{F}^C_{\alpha\beta} + \mathbf{F}^D_{\alpha\beta} + \mathbf{F}^R_{\alpha\beta}) \tag{3}$$

The conservative force is a soft repulsion taking the form as

$$\mathbf{F}^C_{\alpha\beta} = a_{\alpha\beta}\sqrt{\omega(r_{\alpha\beta})}\,\hat{\mathbf{r}}_{\alpha\beta} \tag{4}$$

where $a_{\alpha\beta}$ is the maximum repulsive interaction between particles α and β, $\mathbf{r}_{\alpha\beta} = \mathbf{r}_\alpha - \mathbf{r}_\beta$, $r_{\alpha\beta} = |\mathbf{r}_{\alpha\beta}|$, $\hat{\mathbf{r}}_{\alpha\beta} = \mathbf{r}_{\alpha\beta}/r_{\alpha\beta}$, $\omega(r_{\alpha\beta})$ is the weight function, given by

$$\omega(r_{\alpha\beta}) = \begin{cases} (1 - r_{\alpha\beta}/r_c)^2 & (r_{\alpha\beta} < r_c)\\ 0 & (r_{\alpha\beta} \geq r_c) \end{cases} \tag{5}$$

according to the study by Groot and Warren,[44] and r_c ($r_c = 1.0$) is the cutoff radius. The dissipative force is a friction force that acts on the relative velocities of particles, defined as

$$\mathbf{F}^D_{\alpha\beta} = -\gamma\omega^D(r_{\alpha\beta})(\hat{\mathbf{r}}_{\alpha\beta}\cdot\mathbf{v}_{\alpha\beta})\hat{\mathbf{r}}_{\alpha\beta} \tag{6}$$

and the random force, compensating the loss of kinetic energy due to the dissipative force, is defined as[44]

$$\mathbf{F}^R_{\alpha\beta} = \sigma\omega^R(r_{\alpha\beta})\theta_{\alpha\beta}\hat{\mathbf{r}}_{\alpha\beta} \tag{7}$$

where $\mathbf{v}_{\alpha\beta} = \mathbf{v}_\alpha - \mathbf{v}_\beta$, γ is the friction coefficient, σ is the noise amplitude, $\omega^D(r_{\alpha\beta})$ and $\omega^R(r_{\alpha\beta})$ are weight functions vanishing for $r > r_c$ that describe the range of the dissipative and random forces, and $\theta_{\alpha\beta}$ is a randomly fluctuating variable with Gaussian statistics

$$\langle\theta_{\alpha\beta}(t)\rangle = 0, \qquad \langle\theta_{\alpha\beta}(t)\theta_{kl}(t')\rangle = (\delta_{\alpha k}\delta_{\beta l} + \delta_{\alpha l}\delta_{\beta k})\delta(t-t') \tag{8}$$

In order to satisfy the fluctuation-dissipation theorem and for the system to evolve to an equilibrium state that corresponds to the canonical ensemble, only one of $\omega^D(r_{\alpha\beta})$ and $\omega^R(r_{\alpha\beta})$ can be chosen arbitrarily and the other one is then fixed by the relation[44,46]

$$\omega^D(r_{\alpha\beta}) = [\omega^R(r_{\alpha\beta})]^2 = \omega(r_{\alpha\beta}) \tag{9}$$

And the values of parameters γ and σ are coupled by

$$\sigma^2 = 2\gamma k_B T \tag{10}$$

where k_B and T are the Boltzmann constant and temperature, respectively. In addition, for bonded particles of the multiblock copolymers, the interaction force is considered as the harmonic spring force

$$\mathbf{F}^S_{\alpha\beta} = C(1 - r_{\alpha\beta}/r_{eq})\hat{\mathbf{r}}_{\alpha\beta} \tag{11}$$

In this work, we chose the spring constant $C = 100$ and the equilibrium bond distance $r_{eq} = 0.86$.

In the DPD method, reduced units are adopted for all physical quantities.[44] The units of mass, length, time, and energy are m, r_c, τ, and k_BT, respectively. The time unit τ can be obtained by $\tau = (mr_c^2/k_BT)^{1/2}$. In the simulations, we constructed a coarse-grained model of $A_x(B_yC_z)_n$ multiblock

DOI: 10.1021/la503985u
Langmuir 2015, 31, 2533−2544

copolymers confined between two parallel substrates (denoted by W), separated by a distance Δ, as typically shown in Figure 1. The x, y, z, and n represent the length of A-, B-, and C-blocks

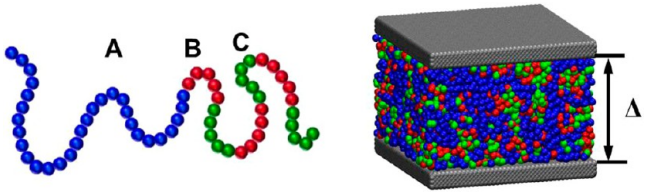

Figure 1. DPD model of $A(BC)_n$ multiblock copolymers confined in thin films with $n = 3$. The blue, red, green, and gray colors are assigned to A, B, C, and substrate (W) particles, respectively. The symbol of Δ represents the film thickness.

and the number of the BC-midblocks, respectively. The two parallel plates are modeled by a set of fixed substrate particles, which are placed at the lattice points of FCC crystal in three layers. The interface contacting with polymer thin films is the (1, 1, 1) surface. The distance between the substrate particles is $0.50r_c$, which is small enough to prevent polymers from penetrating the substrates.

All the simulations were performed in a simulation box of 20 × 20 × Δ, containing 20 × 20 × Δ × 3 DPD beads, where the NVT ensemble and periodic boundary conditions were adopted. The friction coefficient γ and the noise amplitude σ are, respectively, set to be 4.5 and 3.0, and thus, $k_BT = 1.0$. The repulsive parameters for the conservative force between DPD particles are defined so as to produce segregation between A, B, C, and W. They are listed in Table 1. In this work, 3×10^6 DPD steps were carried out so that the computing time is long enough for the system to achieve an equilibrium state.

Table 1. Interaction Parameters $a_{\alpha\beta}$ (in DPD Units) Used in the Simulations

	A	B	C	W
A	25	80−200	80	25
B	80−200	25	400	200
C	80	400	25	200
W	25	200	200	25

2.2. Structure Factor. The structure factor is a mathematical description of how a material scatters incident radiation, which is a particularly useful tool in interpretation of interference patterns obtained in X-ray, electron, and neutron diffraction experiments. In polymer systems, the structure factor is a measure of the correlation between particle positions. To clearly display the layer structure, the structure factor[47,48]

$$S(\mathbf{q}) = \frac{1}{N}\left|\sum_{\beta\neq\alpha} e^{i\mathbf{q}\cdot\mathbf{r}_{\alpha\beta}}\right|^2 \tag{12}$$

was calculated along the X, Y, and Z axes, as well as in the (X, Y), (X, Z), and (Y, Z) planes with the scattering number vector $\mathbf{q}$ being commensurable with the box size, where i is the imaginary unit. All data, except those instant response functions to monitor the structural evolution, were calculated after the system has reached the steady state, as indicated by the fact that the potential energy and pressure tensor components no longer change with time.

2.3. Order Parameter. To measure the order of the structures, we introduced an order parameter S to describe the order degree of the lamellar alignment. The order parameter S_α for the αth normal vector of the domain surface is defined as[49]

$$S_\alpha = \frac{3[\mathbf{u}(\mathbf{r})\cdot\mathbf{u}_d]^2 - 1}{2} \tag{13}$$

$$\mathbf{u}(\mathbf{r}) = \frac{\nabla\varphi_I(\mathbf{r})}{|\nabla\varphi_I(\mathbf{r})|}, \quad I = \text{A, B, or C} \tag{14}$$

where $\varphi_I(\mathbf{r})$ is the density of I-blocks at position $\mathbf{r}$, $\mathbf{u}(\mathbf{r})$ is the αth normal vector of the domain surface, and $\mathbf{u}_d$ is the normalized vector of orientation direction. By choosing different $\mathbf{u}_d$, we can obtain various S, where the S is calculated as the average value of S_α. The order parameter for the domain is determined as the maximum value of S.

3. RESULTS AND DISCUSSION

In this work, we mainly focused on the effect of the film thickness on the microstructures of the multiblock copolymers. The molecular architecture of the multiblock copolymers considered was $A_{30}(B_5C_5)_3$ ($x = 30$, $y = 5$, $z = 5$, and $n = 3$). The two substrates were chosen to be attractive to A-blocks and identically repulsive to B- and C-blocks by setting $a_{AW} = 25$ and $a_{BW} = a_{CW} = 200$. This allows A-blocks to be adsorbed on the surface of the substrates.

The multiblock copolymers can be classified into two categories: one is the nonfrustrated case that the interaction strength between A- and C-blocks is comparable or higher than those between other blocks, and the other is the frustrated case that the A/C interaction strength is smaller than the A/B interaction strength.[13] Therefore, we first undertook a DPD study on these two types of multiblock copolymers in the bulk without confinement. The results were presented in Figure 2.

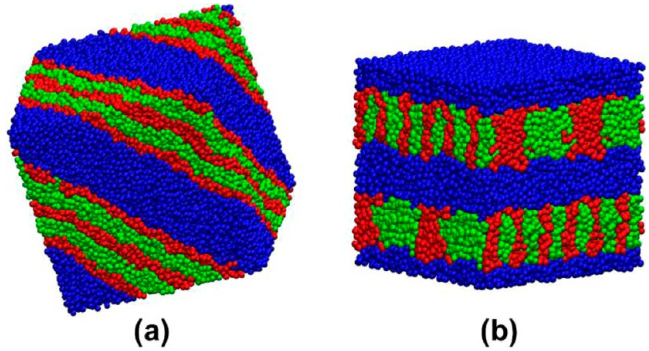

Figure 2. Hierarchical microstructures self-assembled from $A(BC)_3$ multiblock copolymers in the bulk without confinement with $a_{AC} = 80$ and $a_{BC} = 400$: (a) $a_{AB} = 80$ and (b) $a_{AB} = 160$. The blue, red, and green colors are assigned to A, B, and C particles, respectively.

As shown in Figure 2, the multiblock copolymers self-assemble into parallel lamellae-in-lamella ($a_{AB} = 80$, $a_{AC} = 80$, $a_{BC} = 400$, nonfrustrated case, Figure 2a) and perpendicular lamellae-in-lamella ($a_{AB} = 160$, $a_{AC} = 80$, $a_{BC} = 400$, frustrated case, Figure 2b). The results agree well with our previous self-consistent field theory calculations.[13] In contrast to the bulk without confinement, in thin films of each case, hierarchical microstructures with either parallel or perpendicular packed small-length-scale structures could, in principle, be obtained through simply tuning the film thickness.

DOI: 10.1021/la503985u
Langmuir 2015, 31, 2533−2544

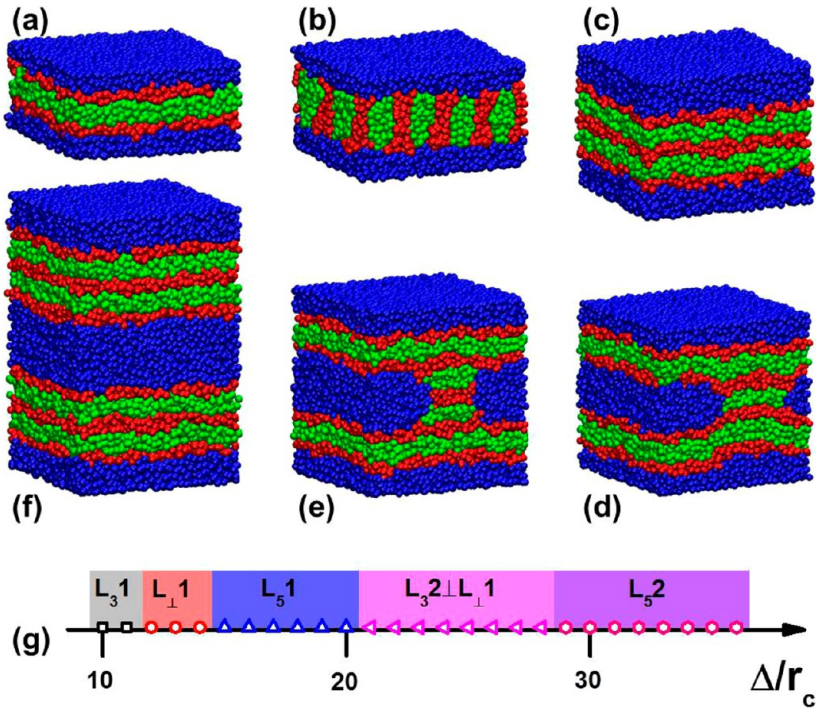

Figure 3. Hierarchical microstructures self-assembled from $A(BC)_3$ multiblock copolymer thin films: (a) $\mathbf{L_3 1}$, (b) $\mathbf{L_\perp 1}$, (c) $\mathbf{L_5 1}$, (d, e) $\mathbf{L_3 2 \perp L_\perp 1}$, and (f) $\mathbf{L_5 2}$. (g) One-dimensional diagram for hierarchical microstructures as a function of Δ/r_c. From parts a to f, the film thickness Δ/r_c is 11, 13, 17, 22, 24, and 32, respectively. The interaction parameters are $a_{AB} = a_{AC} = 80$, $a_{BC} = 400$, $a_{AW} = 25$, and $a_{BW} = a_{CW} = 200$. The blue, red, and green colors are assigned to A, B, and C particles, respectively. The two parallel substrates (wall particles) are omitted.

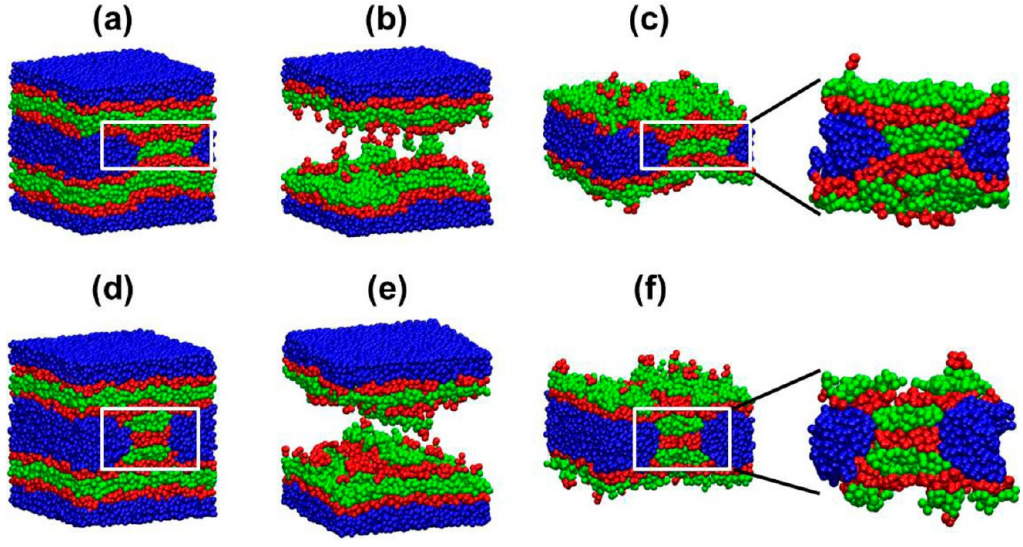

Figure 4. (a, d) Structures formed by all molecules. (b, e) Structures formed by molecules-I whose A-blocks are absorbed to the substrates. (c, f) Structures formed by molecules-II whose A-blocks keep away from the substrates for the coexisting microstructures of $\mathbf{L_3 2 \perp L_\perp 1}$. The coexisting microstructures shown in parts a and d correspond to those in Figure 3d and e, respectively. The blue, red, and green colors are assigned to A, B, and C particles, respectively. The substrate particles are omitted.

3.1. Thin Films of Nonfrustrated Case. We first examined the nonfrustrated system of the $A_{30}(B_5C_5)_3$ multiblock copolymers confined in thin films by setting $a_{AB} = a_{AC} = 80$ and $a_{BC} = 400$. In the bulk without confinement, the parallel lamellae-in-lamellae with five BCBCB-layers are formed (see Figure 2a). However, in the confinement system, the morphologies of hierarchical microstructures become richer. Figure 3 shows the representative lamellae-in-lamellar microstructures observed at various film thicknesses Δ. The beads of A-, B-, and C-blocks are, respectively, denoted with blue, red, and green colors, while the substrate (W) particles are omitted for clarity. As shown in Figure 3, the observed hierarchical lamellae-in-lamellar microstructures include singly periodic parallel lamellae-in-lamella with three BCB-layers ($\mathbf{L_3 1}$, see Figure 3a), singly periodic perpendicular lamellae-in-lamella ($\mathbf{L_\perp 1}$, see Figure 3b), singly periodic parallel lamellae-in-lamella with five BCBCB-layers ($\mathbf{L_5 1}$, see Figure 3c), and doubly periodic parallel lamellae-in-lamella with five BCBCB-layers

DOI: 10.1021/la503985u
Langmuir 2015, 31, 2533−2544

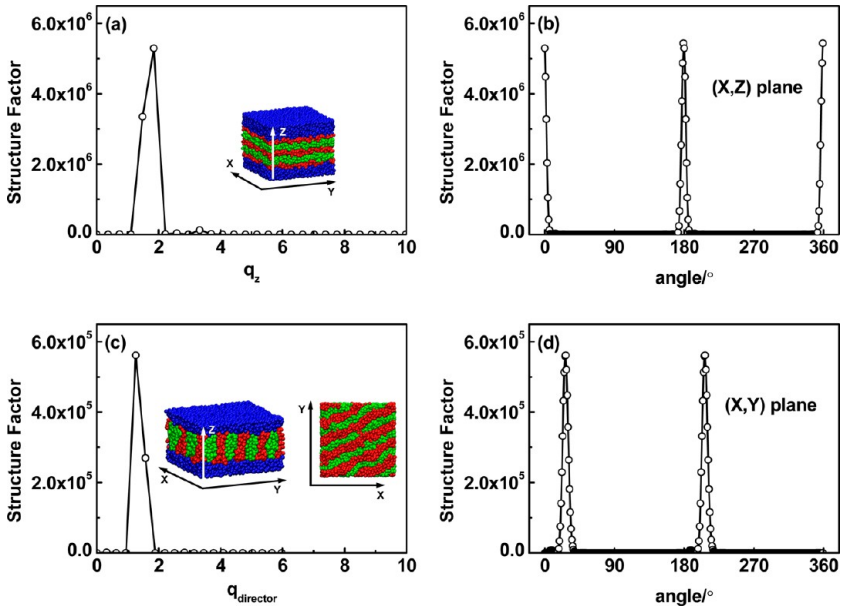

Figure 5. Structure factor scan for the small-length-scale B-layers of $\mathbf{L}_5\mathbf{1}$ (a) as a function of the wave vector $\mathbf{q}$ along the z direction and (b) as a function of angle at $q = q_0$ in the (X, Z) plane. Structure factor scan for the small-length-scale B-layers of $\mathbf{L}_\perp\mathbf{1}$ (c) as a function of the wave vector $\mathbf{q}$ along the director direction and (d) as a function of the angle at $q = q_0$ in the (X, Y) plane.

($\mathbf{L}_5\mathbf{2}$, see Figure 3f). Note that, in the representations such as $\mathbf{L}_3\mathbf{1}$, the first bold letter **L**, subscripts, and last number denote lamellae, the number of the parallel packed small-length-scale lamellae (the symbol $\perp$ means that the small-length-scale lamellae are perpendicular to the large-length-scale lamellae), and the number of the large-length-scale structures, respectively.

Figure 3g displays the one-dimensional phase diagram of the multiblock copolymer thin films as a function of Δ/r_c. When the thin films are very thin ($\Delta/r_c \leq 11$), $\mathbf{L}_3\mathbf{1}$ were observed (Figure 3a). With increasing film thickness ($12 \leq \Delta/r_c \leq 14$), the multiblock copolymers prefer to form perpendicular lamellae-in-lamella, $\mathbf{L}_\perp\mathbf{1}$ (Figure 3b). As the thickness further increases ($15 \leq \Delta/r_c \leq 20$), the microstructures transform to parallel lamellae-in-lamella, but the number of the small-length-scale lamellae increases from three to five. For example, as $\Delta/r_c = 17$, the five parallel alternating BCBCB-layers are parallel to the large-length-scale lamellae formed by A-blocks (see Figure 3c). At a larger value of Δ/r_c ($\geq$29), the periodicity of the large-length-scale lamellae increases and becomes double (see Figure 3f).

In addition, coexistence of two hierarchical microstructures was observed at intermediate thickness ($21 \leq \Delta/r_c \leq 28$). Shown in Figure 3d and e are the coexisting microstructures $\mathbf{L}_3\mathbf{2}\perp\mathbf{L}_\perp\mathbf{1}$. To clarify these coexisting microstructures, the molecular chain distributions in the thin films were further presented, which is shown in Figure 4. The molecules were divided into two categories, according to whether their A-blocks are absorbed to the substrates (molecules-I) or not (molecules-II). It is evident from Figure 4b and e that the B- and C-blocks of molecules-I can hardly stretch to the center of the thin film to form $\mathbf{L}_7\mathbf{1}$ or $\mathbf{L}_9\mathbf{1}$ but to form two domains of $\mathbf{L}_3\mathbf{1}$. From Figure 4c and f, we discovered that the small-length-scale BC-layers in the center of the thin films, marked by white rectangles, are mostly assembled from the B- and C-blocks of molecules-II, indicating that the marked small-length-scale BC-layers are perpendicular to the A-domains self-assembled from A-blocks of molecules-II in the unconfined space to form $\mathbf{L}_\perp\mathbf{1}$. In addition to forming $\mathbf{L}_\perp\mathbf{1}$, the molecules-II join the formation of the $\mathbf{L}_3\mathbf{2}$. Therefore, we denoted these coexisting microstructures as $\mathbf{L}_3\mathbf{2}\perp\mathbf{L}_\perp\mathbf{1}$.

In the thin films of the nonfrustrated case, both the parallel and perpendicular lamellae-in-lamella can be observed by varying the film thickness. To further understand the microstructures, we took one of the parallel lamellae ($\mathbf{L}_5\mathbf{1}$) and perpendicular lamellae ($\mathbf{L}_\perp\mathbf{1}$) as examples to examine the structure factor $S(\mathbf{q})$ of the small-length-scale structures. Figure 5a shows the structure factor $S(\mathbf{q})$ of the vertical configuration along the Z axis for the B-layers in $\mathbf{L}_5\mathbf{1}$. The single peak at $q_0 \approx 1.85$ illustrates the perfect small-length-scale lamellae. The spacing of the small-length-scale lamellae can be calculated by $D = \pi/q_0$, and that is about $1.70r_c$. Then, we calculated the structure factor scanning in the (X, Z) plane for a constant wave length $|\mathbf{q}| = q_0 \approx 1.85$. As exhibited in Figure 5b, two peaks of the same amplitude at 180 and 360° (or 0°) in the (X, Z) plane indicate that the normal of small-length-scale lamellae is along the selected Z direction. For the small-length-scale B-layers of $\mathbf{L}_\perp\mathbf{1}$, a significantly single peak at $q_0 \approx 1.26$ can be found, as shown in Figure 5c. This demonstrates that the small-length-scale lamellae are well aligned. The spacing of the small-length-scale lamellae is $D = \pi/q_0 \approx 2.49r_c$, which is larger than that of $\mathbf{L}_5\mathbf{1}$. Figure 5d shows the structure factor of the small-length-scale B-layers in the (X, Y) plane at a constant wave length $|\mathbf{q}| = q_0 \approx 1.26$. It exhibits two sharp peaks at 27 and 207° (the X direction is the reference direction), indicating that the small-length-scale lamellae are 27 or 207° angle tilted in the (X, Y) plane.

With increasing film thickness, we not only observed the increase of the number of the small-length-scale lamellae but also found a variation of the orientation of the small-length-scale lamellae, e.g., a $\mathbf{L}_3\mathbf{1}$-to-$\mathbf{L}_\perp\mathbf{1}$ phase transition. In bulk without confinement, changing the orientation of the small-length-scale lamellae requires a change of the type of multiblock copolymers (frustrated-to-nonfrustrated). Therefore, it is of significance to understand such a phase transition in thin films. The transition from $\mathbf{L}_3\mathbf{1}$ to $\mathbf{L}_\perp\mathbf{1}$ is due to the fact that the

DOI: 10.1021/la503985u
Langmuir 2015, 31, 2533−2544

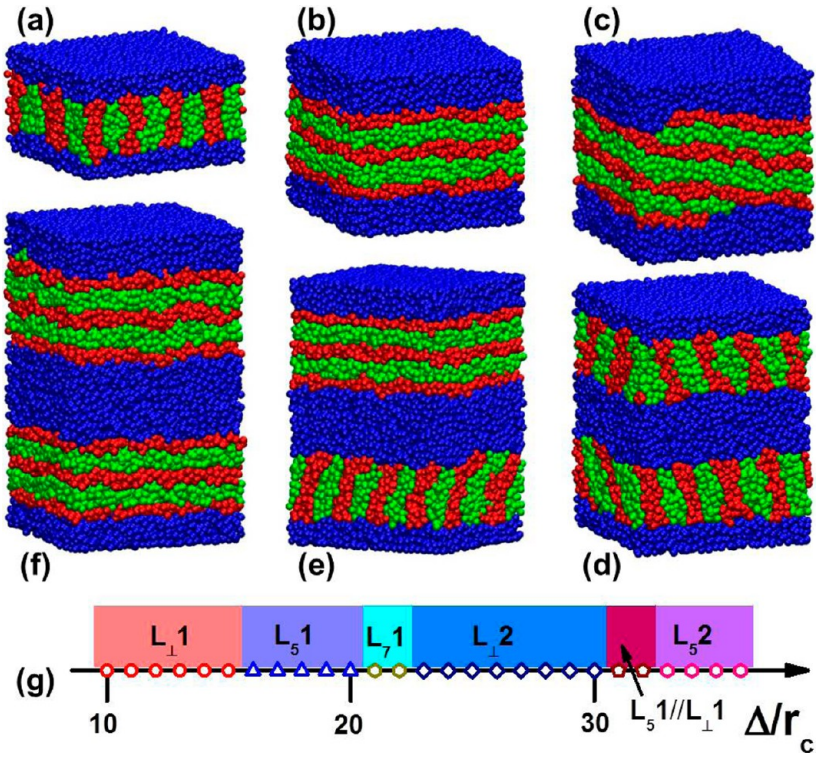

Figure 6. Hierarchical microstructures self-assembled from $A(BC)_3$ multiblock copolymer thin films: (a) $\mathbf{L}_\perp\mathbf{1}$, (b) $\mathbf{L}_5\mathbf{1}$, (c) $\mathbf{L}_7\mathbf{1}$, (d) $\mathbf{L}_\perp\mathbf{2}$, (e) $\mathbf{L}_5\mathbf{1}//\mathbf{L}_\perp\mathbf{1}$, and (f) $\mathbf{L}_5\mathbf{2}$. (g) One-dimensional diagram for hierarchical microstructures as a function of Δ/r_c. From parts a to f, the film thickness Δ/r_c is 13, 19, 21, 28, 32, and 36, respectively. The interaction parameters are $a_{AB} = 160$, $a_{AC} = 80$, $a_{BC} = 400$, $a_{AW} = 25$, and $a_{BW} = a_{CW} = 200$. The colors appear as in Figure 3. The substrate particles are omitted.

thickness is highly incommensurate with the period of the three-layered small-length-scale structures. Through forming $\mathbf{L}_\perp\mathbf{1}$, the frustrations of B- and C-chains within small-length-scale structures can be relieved, since the perpendicular arrangement of small-length-scale lamellae allows the layers to retain their bulk period. However, the $\mathbf{L}_\perp\mathbf{1}$ cannot be maintained to a large value of film thickness. This is because the B- and C-chains must be highly stretched normal to the large-length-scale lamellae in order to fill the domains of the extended small-length-scale lamellae. To alleviate such chain frustration, parallel hierarchical lamellae with more small-length-scale lamellae are formed. In these morphological transformations, the surface energy becomes less favorable, but the entropy is favored. As the film becomes thicker, the film thickness approaches the double period of $\mathbf{L}_3\mathbf{1}$ and thus the double periodic hierarchical lamellae are formed instead of single periodic hierarchical lamellae with more small-length-scale lamellae. However, before forming well-defined doubly periodic microstructures, the coexistence of two hierarchical microstructures $\mathbf{L}_3\mathbf{2}\perp\mathbf{L}_\perp\mathbf{1}$ appears.

To examine whether the $\mathbf{L}_3\mathbf{2}\perp\mathbf{L}_\perp\mathbf{1}$ microstructures are in equilibrium or not, we carried out a further study on the $\mathbf{L}_3\mathbf{2}\perp\mathbf{L}_\perp\mathbf{1}$ microstructures at various XY-spaces. Note that the time step was set to 3×10^6 which is long enough to achieve an equilibrium state. The simulation results for $\Delta/r_c = 22$ and $\Delta/r_c = 24$ are shown in Figure S1 in the Supporting Information. The influence of the size of the unconfined X- and Y-space, L_X and L_Y, was demonstrated. It was found that the $\mathbf{L}_3\mathbf{2}\perp\mathbf{L}_\perp\mathbf{1}$ stays unchanged and cannot be relaxed to $\mathbf{L}_3\mathbf{2}$ or $\mathbf{L}_\perp\mathbf{2}$ as L_X and L_Y varies. This suggests that the $\mathbf{L}_3\mathbf{2}\perp\mathbf{L}_\perp\mathbf{1}$ microstructures are in equilibrium essentially. The physical origin that the $\mathbf{L}_3\mathbf{2}\perp\mathbf{L}_\perp\mathbf{1}$ structures appear at certain film thickness can be explained as follows. At a certain film thickness, for example, $\Delta/r_c = 22$, the free energies cannot be minimized by forming either the double $\mathbf{L}_3\mathbf{1}$ (or $\mathbf{L}_3\mathbf{2}$) or the double $\mathbf{L}_\perp\mathbf{1}$ (or $\mathbf{L}_\perp\mathbf{2}$). The entropy is unfavorable in $\mathbf{L}_3\mathbf{2}$, and the enthalpy is unfavorable in $\mathbf{L}_\perp\mathbf{2}$. However, through forming $\mathbf{L}_3\mathbf{2}\perp\mathbf{L}_\perp\mathbf{1}$, the entropy is gained compared with $\mathbf{L}_3\mathbf{2}$ and the enthalpy is reduced compared with $\mathbf{L}_\perp\mathbf{2}$. Finally, the free energy is minimized in $\mathbf{L}_3\mathbf{2}\perp\mathbf{L}_\perp\mathbf{1}$. The appearance of these nonlamellar structures is essentially consistent with the emergence of the coexistence of parallel and perpendicular lamellae in the thin films of lamella-forming diblock copolymers.[33] At much larger Δ, the $\mathbf{L}_5\mathbf{2}$ are formed and the coexisting hierarchical microstructures do not emerge.

At the end of this subsection, we would like to remark on the a_{BC}-parameter. Because the value of a_{BC} is relatively larger, we wondered if such a large value of the parameter can reflect correct physics. To make a comparison, we have carried out an additional simulation on the $A(BC)_3$ multiblock copolymer thin films with smaller values of $a_{BC} = 200$. The results were presented in Figure S2 in the Supporting Information. Figure S2 shows the representative hierarchical microstructures self-assembled from $A(BC)_3$ multiblock copolymer thin films with $a_{AB} = a_{AC} = 80$, $a_{AW} = 25$, $a_{BW} = a_{CW} = 200$, and $a_{BC} = 200$ at various Δ. Similar to the nonfrustrated case with $a_{BC} = 400$, the hierarchical microstructures including $\mathbf{L}_3\mathbf{1}$ (Figure S2a, Supporting Information), $\mathbf{L}_\perp\mathbf{1}$ (Figure S2b, Supporting Information), $\mathbf{L}_5\mathbf{1}$ (Figure S2c, Supporting Information), $\mathbf{L}_3\mathbf{2}\perp\mathbf{L}_\perp\mathbf{1}$ (Figure S2d,e, Supporting Information), and $\mathbf{L}_5\mathbf{2}$ (Figure S2f, Supporting Information) were observed. Figure S2g (Supporting Information) displays the one-dimensional phase diagram of $A(BC)_3$ multiblock copolymer thin films as a function of Δ/r_c. Comparing with the nonfrustrated case with $a_{BC} = 400$, the morphological transformation in the sequence of

DOI: 10.1021/la503985u
Langmuir 2015, 31, 2533−2544

$\mathbf{L_3 1}$, $\mathbf{L_\perp 1}$, $\mathbf{L_5 1}$, $\mathbf{L_3 2 \perp L_\perp 1}$, and $\mathbf{L_5 2}$ and the transition boundaries are the same except for the transition boundary between $\mathbf{L_5 1}$ and $\mathbf{L_3 2 \perp L_\perp 1}$ which shows a shift toward larger Δ. We noticed no qualitative difference in the simulated results for a_{BC} = 200 (Figure S2, Supporting Information) and a_{BC} = 400 (Figure 3). As a matter of fact, the B- and C-blocks are not strongly separated at a_{BC} = 400. Taking the perpendicular lamellae-in-lamella (see Figure 3b) as an example, the order parameter S_{BC} is about 0.57 (S_{BC} = 0 and 1 respectively represent disorder and complete separation), indicating that the separation between B- and C-blocks is relatively weaker. These results indicate that the simulation for a higher value of a_{BC} = 400 can reflect correct physics.

3.2. Thin Films of Frustrated Case. In this case, the molecular interaction parameters are set as a_{AB} = 160, a_{AC} = 80, and a_{BC} = 400. In the bulk without confinement, the perpendicular lamellae-in-lamellae are favored (see Figure 2b). Figure 6 shows the representative hierarchical lamellae obtained at various film thicknesses. Similar to the nonfrustrated cases, the hierarchical microstructures including $\mathbf{L_\perp 1}$, $\mathbf{L_5 1}$, $\mathbf{L_7 1}$, $\mathbf{L_\perp 2}$, and $\mathbf{L_5 2}$ were observed. Shown in Figure 6g is the one-dimensional phase diagram. As can be seen, when the films are relatively thin ($\Delta/r_c \leq 15$), only the $\mathbf{L_\perp 1}$ (see Figure 6a) are formed. Ranging from Δ/r_c = 16 to Δ/r_c = 20, the parallel lamellae-in-lamellae with five BCBCB-layers ($\mathbf{L_5 1}$, see Figure 6b) are favored. With an increase in Δ/r_c from 21 to 22, the $\mathbf{L_7 1}$ are observed, as shown in Figure 6c. The doubly periodic lamellae-in-lamellae $\mathbf{L_\perp 2}$ (Figure 6d) and $\mathbf{L_5 2}$ (Figure 6f) are formed at $23 \leq \Delta/r_c \leq 30$ and $\Delta/r_c \geq 33$, respectively. In the region of the transformation from $\mathbf{L_\perp 2}$ to $\mathbf{L_5 2}$, a coexistence of two hierarchical lamellae of $\mathbf{L_5 1 // L_\perp 1}$ (see Figure 6e) emerges. The structural transformation is similar to the nonfrustrated case, where the multiblock copolymers self-assemble into singly periodic hierarchical lamellae at small thickness and doubly periodic hierarchical lamellae at large thickness.

The structural transformation of $\mathbf{L_\perp 1} \rightarrow \mathbf{L_5 1} \rightarrow \mathbf{L_7 1} \rightarrow \mathbf{L_\perp 2} \rightarrow \mathbf{L_5 1 // L_\perp 1} \rightarrow \mathbf{L_5 2}$ is also due to the mismatch between the periodicity of the small-length-scale structures and the film thickness. A more remarkable phenomenon is the appearance of the coexistence of hierarchical lamellae, i.e., $\mathbf{L_5 1 // L_\perp 1}$. The entropy in the coexisting hierarchical lamellae can be more favorable than those in either doubly periodic $\mathbf{L_\perp 2}$ or doubly periodic $\mathbf{L_5 2}$. The case is different from the coexisting microstructures of $\mathbf{L_3 2 \perp L_\perp 1}$ observed in the nonfrustrated case (see Figure 3d and e). The microstructures in Figure 3d and e are the coexistence of parallel and perpendicular lamellae where they are perpendicular, while the present microstructures are the coexistence of parallel and perpendicular lamellae where they are parallel with each other. The appearance of the different orientations of the coexisting structures is due to the difference in the (frustrated and nonfrustrated) cases. The formation of the former one can effectively reduce the ratio of perpendicular lamellae as compared to the latter one, and vice versa, because the perpendicular hierarchical lamellae are unfavorable in the bulk of the former one but are favored in the bulk of the latter one.

To illustrate the effect of the interaction strength between different blocks, the morphological stable regions in a_{AB}–Δ space were mapped out for the thin films of $A_{30}(B_5C_5)_3$ multiblock copolymers, which is shown in Figure 7. The a_{AC} and a_{BC} were fixed as 80 and 400, respectively. As a_{AB} increases from 80 to 200, the systems are transformed from the nonfrustrated case to the frustrated case. In the diagram, each point corresponds to a simulation result. The blue and yellow regions include the singly and doubly periodic microstructures, respectively. It can be seen that the film thickness has a marked influence on the microstructures. The boundary between singly and doubly periodic lamellae shows a shift to a higher value of Δ as a_{AB} increases, indicating that the domain size increases as a_{AB} increases. From the phase diagram, we found that the parallel hierarchical lamellae with three BCB-layers ($\mathbf{L_3 1}$) are only stable when a_{AB} is less than or equal to a_{AC}. In addition, the phase boundary between $\mathbf{L_\perp 1}$ and $\mathbf{L_5 1}$ shifts toward higher Δ as a_{AB} increases, implying that the $\mathbf{L_5 1}$ can transform to $\mathbf{L_\perp 1}$ with increasing a_{AB} within a special range of Δ/r_c, as indicated by the arrow in Figure 7. Such phase behaviors can be rationalized by considering the interfacial energy. The increase in a_{AB} induces a greater increase in interfacial energy of $\mathbf{L_5 1}$ than that of $\mathbf{L_\perp 1}$ due to the large area of A/B interfaces, leading to a shift of phase boundary between $\mathbf{L_\perp 1}$ and $\mathbf{L_5 1}$ to larger Δ/r_c.

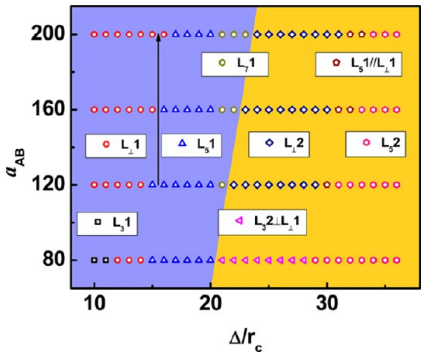

Figure 7. Observed microstructure regions as a function of Δ/r_c at various a_{AB} for the $A(BC)_3$ multiblock copolymer thin film with a_{AC} = 80, a_{BC} = 400, a_{AW} = 25, and a_{BW} = a_{CW} = 200. The blue and yellow regions include the singly and doubly periodic microstructures, respectively.

3.3. Formation Dynamics of Hierarchical Microstructures in Thin Films. The dynamics of hierarchical microstructure formation was further studied. The study was first focused on two representative hierarchical microstructures: one is perpendicular lamellae-in-lamella $\mathbf{L_\perp 1}$, and the other is parallel lamellae-in-lamella $\mathbf{L_5 1}$. The representative morphological evolutions were presented in Figure 8. The formation of $\mathbf{L_\perp 1}$ exhibits an obvious two-step self-assembly, as shown in Figure 8a. At the initial stage (e.g., $t = 2000\tau$), the A-blocks are rapidly absorbed to the hard substrates, forming well-aligned large-length-scale layers. However, the small-length-scale structures formed by B- and C-blocks are still not well formed. As time goes, the small-length-scale lamellae become ordered. Thus, in the self-assembly of $\mathbf{L_\perp 1}$, the large-length-scale structures are first formed, and then the small-length-scale structures are gradually formed. The formation process of $\mathbf{L_5 1}$ is similar to that of $\mathbf{L_\perp 1}$, as shown in Figure 8b. At the initial stage (e.g., $t = 2000\tau$), neither the large-length-scale structures nor the small-length-scale structures are ordered. Note that the small-length-scale structures are almost perpendicular to the large-length-scale A-domains. This implies that the initial self-assembly performs as that in the bulk, since the bulk system favors perpendicular hierarchical microstructures (see Figure 2b). As the A-blocks are perfectly absorbed to the substrates ($t = 6000\tau$), the small-length-scale structures become parallel to the large-length-scale A-domains to adjust the BC-chains to

DOI: 10.1021/la503985u
Langmuir 2015, 31, 2533−2544

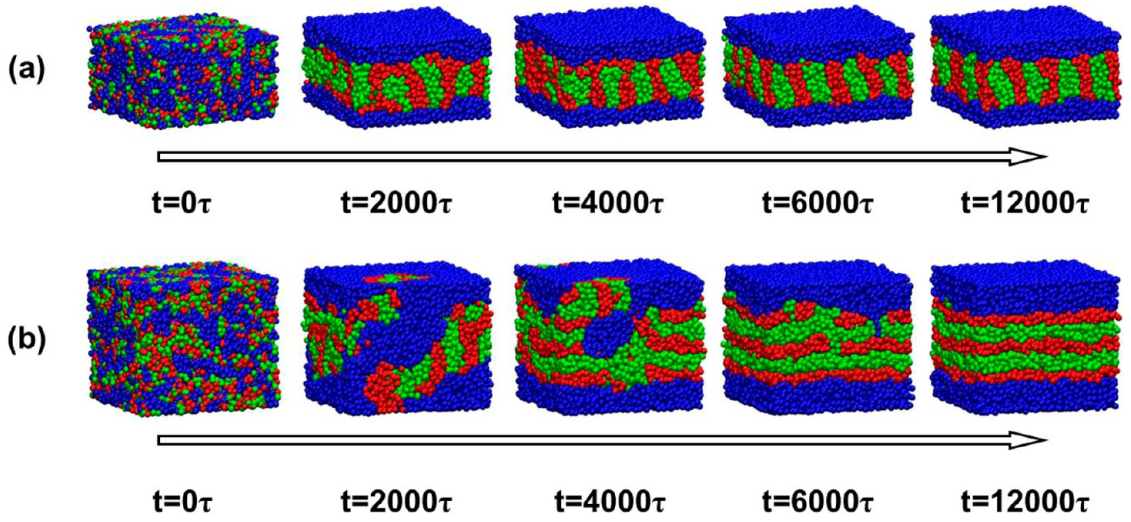

Figure 8. Dynamic process of the formation of (a) $\mathbf{L}_{\perp}\mathbf{1}$ in Figure 6a and (b) $\mathbf{L}_{S}\mathbf{1}$ in Figure 6b for the $A(BC)_3$ multiblock copolymer thin films at different times. The interaction parameters are the same as those in Figure 6. The colors appear as in Figure 3. The substrate particles are omitted.

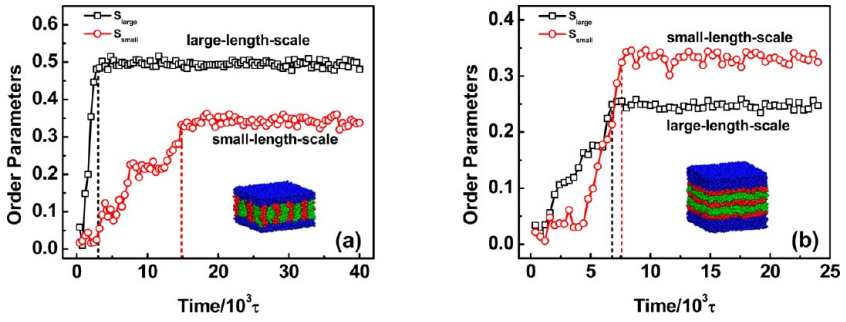

Figure 9. Order parameters of the normal vectors of the A-domain surfaces (black line with squares, S_{large}) and interfaces between B- and C-domains (red line with circles, S_{small}) for (a) $\mathbf{L}_{\perp}\mathbf{1}$ and (b) $\mathbf{L}_{S}\mathbf{1}$ with $a_{AB} = 160$, $a_{AC} = 80$, $a_{BC} = 400$, $a_{AW} = 25$, and $a_{BW} = a_{CW} = 200$. S_{large} and S_{small} represent the ordering of the large-length-scale and small-length-scale structures, respectively. The insets in parts a and b show the corresponding hierarchical microstructures.

accommodate the confined space. Compared with the formation of well-defined large A-domains, the ordering of the small-length-scale structures was delayed slightly. With time going, the well-arranged $\mathbf{L}_{S}\mathbf{1}$ is finally formed.

To further understand the formation dynamics of $\mathbf{L}_{\perp}\mathbf{1}$ and $\mathbf{L}_{S}\mathbf{1}$, we calculated the order parameters of different-length-scale structures. The results are shown for $\mathbf{L}_{\perp}\mathbf{1}$ and $\mathbf{L}_{S}\mathbf{1}$ in Figure 9, where the order parameters of the normal vectors of the A-domain surfaces (black line with squares, S_{large}) and interfaces between B- and C-domains (red line with circles, S_{small}) represent the ordering of the large-length-scale and small-length-scale structures, respectively. As can be seen from Figure 9a ($\mathbf{L}_{\perp}\mathbf{1}$), the S_{large} increases rapidly to a plain region at time $t = 2800\tau$, while the S_{small} rises slowly until it reaches a steady value of 0.34 at time $t = 14800\tau$. It suggests that the well-defined large-length-scale structures and small-length-scale structures are settled at time $t = 2800\tau$ and $t = 14800\tau$, respectively. In other words, the formation of $\mathbf{L}_{\perp}\mathbf{1}$ shows a two-step self-assembly behavior, as also observed from Figure 8a. In Figure 9b ($\mathbf{L}_{S}\mathbf{1}$), both the S_{large} and S_{small} increase and finally level off at time $t = 6800\tau$ and $t = 7600\tau$, respectively. It means that, for $\mathbf{L}_{S}\mathbf{1}$, the formation of the large-length-scale structures is a little faster than that of the small-length-scale structures.

In addition to the hierarchical microstructures mentioned above, we also observed some other microstructures where two hierarchical microstructures are coexisting. The formation dynamics of these coexisting hierarchical microstructures was studied. The results were presented in Figure 10. Figure 10a shows the formation pathway of the coexisting microstructures $\mathbf{L}_{S}\mathbf{1}//\mathbf{L}_{\perp}\mathbf{1}$ where the parallel microstructures ($\mathbf{L}_{S}\mathbf{1}$) and perpendicular microstructures ($\mathbf{L}_{\perp}\mathbf{1}$) are parallel with each other. With time going, partial A-blocks are adsorbed to the substrates and the remainders stay in the body of the systems (from time $t = 0\tau$ to 16000τ). However, the A-domains in the body are not in the center but close to one side of the substrates, dividing the BC-domains into an upper large space and a lower small space (e.g., $t = 4000\tau$, 8000τ, and 16000τ). The small-length-scale lamellae formed by the BC-blocks tend to be parallel to the A-domains within the upper large space and perpendicular to the A-domains within the lower small space ($t = 8000\tau$ and 16000τ). In addition, the A-domains in the body are still not well-arranged and some defected cavities are observed. Within the cavities, the small-length-scale structures formed by the BC-blocks are perpendicular to the neighboring A-domains ($t = 8000\tau$ and 16000τ). As time goes, the defected microstructures are gradually absorbed into lower perpendicular hierarchical lamellae and the small-length-scale lamellae become well-aligned at time $t = 28000\tau$. The confined systems finally self-assemble into the coexisting hierarchical microstructures consisting of parallel lamellae ($\mathbf{L}_{S}\mathbf{1}$) in the upper large space and perpendicular lamellae ($\mathbf{L}_{\perp}\mathbf{1}$) in the lower small space. From Figure 10a, we can see that the

DOI: 10.1021/la503985u
Langmuir 2015, 31, 2533−2544

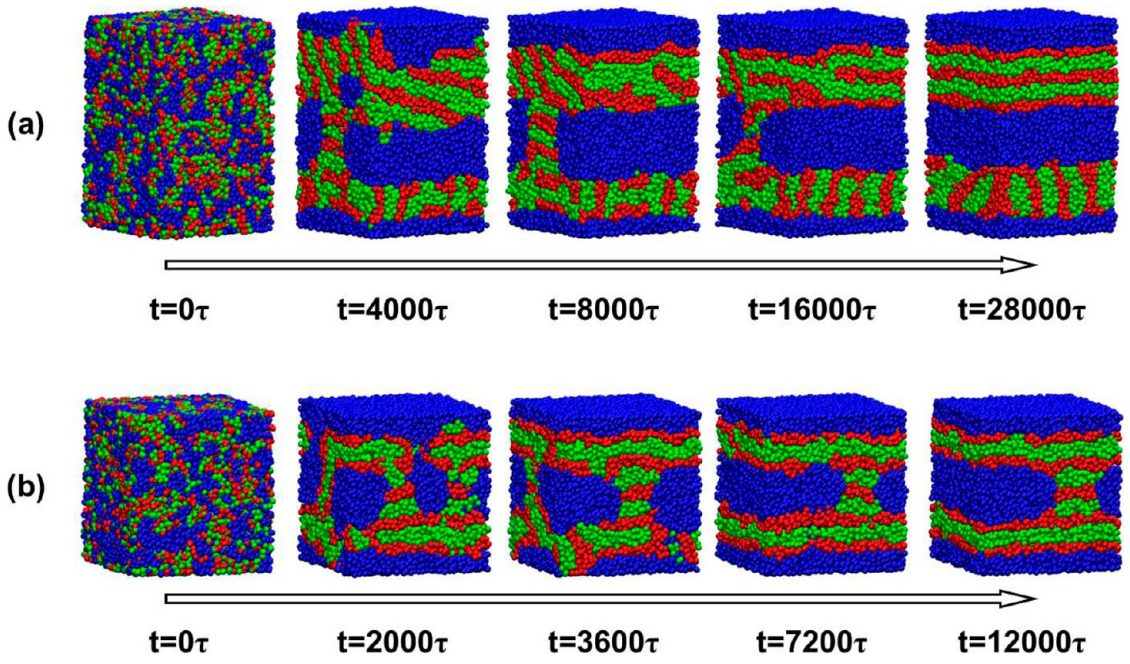

Figure 10. Dynamic process of the formation of (a) $\mathbf{L}_5\mathbf{1}//\mathbf{L}_\perp\mathbf{1}$ in Figure 6e and (b) $\mathbf{L}_3\mathbf{2}\perp\mathbf{L}_\perp\mathbf{1}$ in Figure 3e for the $A(BC)_3$ multiblock copolymer thin films at different times. The interaction parameters for parts a and b are the same as those in Figures 6 and 3, respectively. The colors appear as in Figure 3. The substrate particles are omitted.

ordering of small-length-scale lamellae changes followed by the variation of large-length-scale lamellae, and thereby the formation of well-aligned small-length-scale lamellae always lags behind that of well-aligned A-domains.

Shown in Figure 10b is the formation of the coexisting microstructures of $\mathbf{L}_3\mathbf{2}\perp\mathbf{L}_\perp\mathbf{1}$ where the parallel microstructures ($\mathbf{L}_3\mathbf{2}$) are perpendicular to the perpendicular microstructures ($\mathbf{L}_\perp\mathbf{1}$). As time goes, the A-domains, which are adsorbed to the substrates and remain in the body, are first formed (from time $t = 0\tau$ to 7200τ). Different from $\mathbf{L}_5\mathbf{1}//\mathbf{L}_\perp\mathbf{1}$ in Figure 10a, the A-domains in the body are nearly in the center between two substrates (e.g., $t = 2000\tau$, 3600τ, and 7200τ). The BC-blocks then form small-length-scale structures to adapt to the large-length-scale A-domains. The BC-blocks near the substrates tend to form lamellae parallel to the A-domains ($t = 3600\tau$ and 7200τ). In the center A-domains, some defected cavities exist and the BC-blocks form lamellae perpendicular to the neighboring A-domains ($t = 3600\tau$ and 7200τ). With time going, the cavities are fused and ultimately form one perpendicular hierarchical lamella within the center A-domains at time $t = 12000\tau$. This lamella cannot be absorbed into the parallel hierarchical lamellae, and therefore, the coexistence of two hierarchical microstructures appears. It can be concluded from Figures 8−10 that, in the self-assembly of the multiblock copolymers in thin films, the large-length-scale structures are first formed and then the small-length-scale structures are adjusted to accommodate the large-length-scale structures.

3.4. Comparison with Existing Observations. In the thin films of multiblock copolymers, the A-blocks are absorbed to the hard substrates and form wetting surfaces for the remaining $(BC)_n$-blocks to phase separate. Therefore, the formation of the small-length-scale structures can be regarded as the phase separation of block copolymers in thin films confined between two soft walls. Many experiments and theories have dealt with the thin films of block copolymers such as diblock copolymers.[14−34] For example, Russell et al. investigated the self-assembly of diblock copolymers in thin films, and found that the lamellae parallel or perpendicular to the thin films can alternatively appear and the number of the lamellae increases with increasing film thickness.[30,31] This is because the chain frustration in parallel lamellae can be relieved by forming perpendicular lamellae, although the latter has a less favorable surface energy. In this work, we also found that the small-length-scale structures can be transformed between perpendicular lamellae and parallel lamellae, resulting in various hierarchical lamellae with either parallel or perpendicular packed small-length-scale lamellae (see Figure 6). Moreover, the number of the small-length-scale lamellae increases as the film thickness increases. Thus, the self-assembly of the small-length-scale structures within large-length-scale structures is essentially consistent with the phase separation of the thin films of diblock copolymers.

However, the self-assembly of multiblock copolymers between two surfaces shows distinctive phase behavior that is unrevealed in conventional block copolymer thin films. First, for the nonfrustrated case, the surface wetting by A-blocks exhibits no preference toward B- and C-blocks, since $a_{AB} = a_{BC}$, and therefore, it can be compared with the lamella-forming diblock copolymers confined between two nonselective surfaces. With increased film thickness, the perpendicular lamellae are always stable for the diblock copolymer films. However, for the multiblock copolymer films, the small-length-scale lamellae undergo perpendicular-to-parallel transition by changing the film thickness. The emergence of either parallel or perpendicular lamellae is due to entropic reasons, because one end of the B-blocks is connected to the A-blocks. Second, for selective surfaces, the perpendicular lamellae in thin films of diblock copolymers can emerge alternatively as long as the surface repulsion is not too large. However, in the thin films of frustrated multiblock copolymers, the perpendicular hierarchical lamellae only appear at small film thickness. (Note that, although the perpendicular lamellae with double periodicities

DOI: 10.1021/la503985u
Langmuir 2015, 31, 2533−2544

can be formed at a relative large film thickness, their periodicity is also increased.) This may be due to the fact that the large values of a_{AB} and a_{AC} are chosen to ensure the phase separation between A- and B/C-blocks. Third, the number of the layers in parallel lamellae of diblock copolymer films can continuously increase as the film thickness increases. However, in our simulations, the number of the small-length-scale lamellae in hierarchical lamellae is limited, since the $(BC)_n$-blocks are connected to the A-blocks. Instead of single periodic hierarchical lamellae with more small-length-scale lamellae, doubly periodic hierarchical lamellae are formed. The distinctive phase behavior of the multiblock copolymers in thin films can enrich the knowledge about the self-assembly of block copolymers in thin films.

There are no direct experimental studies on controllable hierarchical microstructures of such multiblock copolymer thin film systems, and therefore, it is difficult to make a direct comparison between theoretical predictions and experimental observations. However, there are still some existing experimental observations regarding the hierarchical microstructures self-assembled from copolymer in thin films in the literature to support our simulation results. For example, comb-shaped supramolecules are a system capable of forming hierarchical microstructures. In bulk, both the multiblock copolymers and comb-shaped supramolecules can form hierarchical microstructures with similar arrangements, for example, parallel lamellae-in-lamellae and perpendicular lamellae-in-lamellae.[13,50] Therefore, in the present work, we utilized the results obtained from comb-shaped supramolecules to make a comparison with our predictions in terms of the hierarchical microstructures. ten Brinke and co-workers have examined the phase behavior and terrace formation of solvent vapor annealed thin films of asymmetric comb-shaped supramolecules consisting of a polystyrene (PS) block and a supramolecular block of poly(4-vinylpyridine) (P4VP) hydrogen bonded with pentadecylphenol (PDP) on silicon oxide.[51] It was found that the lowest terrace consisted of two wetting layers forming one lamella, the second terrace contained perpendicular lamellae, and the highest terrace consisted of parallel P4VP(PDP) cylinders. Below the order−disorder transition temperature, the P4VP(PDP) combs form alternating layers of P4VP and PDP, and the thin films of hierarchical microstructures are obtained. The experimental results were presented in a morphology transformation as a function of film thickness: the morphologies transform from perpendicular hierarchical microstructures to parallel hierarchical microstructures and then to perpendicular hierarchical microstructures as the film thickness increases. This is consistent with our calculations that the morphologies of the multiblock copolymer thin films undergo a formation evolution from $\mathbf{L}_\perp\mathbf{1} \rightarrow \mathbf{L}_5\mathbf{1} \rightarrow \mathbf{L}_7\mathbf{1} \rightarrow \mathbf{L}_\perp\mathbf{2}$ as the film thickness increases (see Figure 6). The present simulation results realized the controllable manufacture of the hierarchical morphologies and also offered a direction of preparing thin films with different hierarchical microstructures.

The thin films with controllable orientation and number of the small-length-scale lamellae can afford a facile route to generate hierarchical microstructures. The thin films may find many applications in fabricating functional nanodevices, for example, integrated circuit devices. In industry integrated circuit design, fabrication of nonperiodic structures such as T-junctions (a structure like capital "T") and jogs is especially crucial.[52] A conventional way for block copolymer lithography to fabricate nonperiodic structures is to devise confinement/patterning strategies for block copolymer films. In this work, we proposed an alternative for producing structures with nonperiodic features like T-junctions without devising confinement/patterning strategies. Here, we introduced $A(BC)_n$ multiblock copolymers that are capable of forming hierarchical structures within two solid surfaces (to date, little is known for the microphase separation of multiblock copolymers confined between two solid surfaces). For example, the perpendicular packed hierarchical lamellae, containing various T-junction structures (for example, combining A- and B-domains and cutting along the center line between substrates), can meet the need for fabricating T-junctions in circuit devices. Since the perpendicular packed hierarchical lamellae can be readily obtained by regulating the film thickness, the thin films of multiblock copolymers could be harnessed in a variety of ways. In the applications, control of orientation and domain order can also be achieved by tuning the film thickness. Beyond that, the thin films described here can also offer many opportunities to fabricate other functional devices, and the fundamental principle for producing a series of hierarchical microstructures could be potentially applicable to other polymer systems.

4. CONCLUSIONS

We employed the dissipative particle dynamics simulations to investigate the hierarchical microstructures self-assembled from $A(BC)_n$ multiblock copolymers in thin films, where the thin films are confined between two solid substrates selective for A-blocks. Two cases were examined according to the relative interaction strength: one is the nonfrustrated case that $a_{AB} \leq a_{AC}$, and the other is the frustrated case that $a_{AB} > a_{AC}$. For both cases, either parallel or perpendicular lamellae-in-lamellae were found. Not only can the periodicity of the large-length-scale structures change from single to double, but the small-length-scale structures also undergo a parallel-to-perpendicular transition as Δ changes. As Δ increases, a morphological transformation in the sequence of $\mathbf{L}_3\mathbf{1}$, $\mathbf{L}_\perp\mathbf{1}$, $\mathbf{L}_5\mathbf{1}$, $\mathbf{L}_3\mathbf{2}\perp\mathbf{L}_\perp\mathbf{1}$, and $\mathbf{L}_5\mathbf{2}$ was observed for the nonfrustrated case, and a structural transformation of $\mathbf{L}_\perp\mathbf{1} \rightarrow \mathbf{L}_5\mathbf{1} \rightarrow \mathbf{L}_7\mathbf{1} \rightarrow \mathbf{L}_\perp\mathbf{2} \rightarrow \mathbf{L}_5\mathbf{1}//\mathbf{L}_\perp\mathbf{1} \rightarrow \mathbf{L}_5\mathbf{2}$ was found for the frustrated case. In addition to the well-defined hierarchical microstructures, novel coexisting hierarchical microstructures such as $\mathbf{L}_3\mathbf{2}\perp\mathbf{L}_\perp\mathbf{1}$ and $\mathbf{L}_5\mathbf{1}//\mathbf{L}_\perp\mathbf{1}$ were discovered. In the coexisting hierarchical microstructures, two hierarchical microstructures can be either parallel or perpendicular with each other. As a_{AB} increases, the boundaries for the transitions of single-to-double periodicity and perpendicular-to-parallel arrangement show a shift toward larger Δ. The dynamics of the hierarchical microstructure formation was also studied. It was found that the formation of small-length-scale structures always lags behind that of large-length-scale structures. The results could provide the guidance for preparing thin films with diversified, controllable hierarchical microstructures.

■ ASSOCIATED CONTENT

Supporting Information

Size effect (simulation space) on the coexisting microstructures and studies on the thin films of the nonfrustrated case with a_{BC} = 200. This material is available free of charge via the Internet at http://pubs.acs.org.

■ AUTHOR INFORMATION

Corresponding Authors

*Phone: +86-21-64251615. E-mail: lq_wang@ecust.edu.cn.

DOI: 10.1021/la503985u
Langmuir 2015, 31, 2533−2544

*Phone: +86-21-64253370. E-mail: jlin@ecust.edu.cn.

Notes

The authors declare no competing financial interest.

■ ACKNOWLEDGMENTS

This work was supported by National Natural Science Foundation of China (21304035, 21234002), Key Grant Project of Ministry of Education (313020), National Basic Research Program of China (No. 2012CB933600), Fundamental Research Funds for the Central Universities (222201314024), and Research Fund for the Doctoral Program of Higher Education of China (20120074120002). Support from project of Shanghai municipality (13JC1402000) is also appreciated.

■ REFERENCES

(1) Sanchez, C.; Arribart, H.; Guille, M. M. G. Biomimetism and Bioinspiration as Tools for the Design of Innovative Materials and Systems. *Nat. Mater.* **2005**, *4*, 277−288.
(2) Tang, Z.; Kotov, N. A.; Magonov, S.; Ozturk, B. Nanostructured Artificial Nacre. *Nat. Mater.* **2003**, *2*, 413−418.
(3) Lakes, R. Materials with Structural Hierarchy. *Nature* **1993**, *361*, 511−515.
(4) Zeng, X.; Ungar, G.; Liu, Y.; Percec, V.; Dulcey, A. E.; Hobbs, J. K. Supramolecular Dendritic Liquid Quasicrystals. *Nature* **2004**, *428*, 157−160.
(5) Vaia, R.; Baur, J. Adaptive Composites. *Science* **2008**, *319*, 420−421.
(6) Sanchez, C.; Boissiere, C.; Grosso, D.; Laberty, C.; Nicole, L. Design, Synthesis, and Properties of Inorganic and Hybrid Thin Films Having Periodically Organized Nanoporosity. *Chem. Mater.* **2008**, *20*, 682−737.
(7) Ma, X.; Xia, Y.; Chen, E.-Q.; Mi, Y.; Wang, X.; Shi, A.-C. Crust Effect on Multiscale Pattern Formations in Drying Micelle Solution Drops on Solid Substrates. *Langmuir* **2004**, *20*, 9520−9525.
(8) Xu, W.; Liu, H.; Lu, S.; Xi, J.; Wang, Y. Fabrication of Superhydrophobic Surfaces with Hierarchical Structure through a Solution-Immersion Process on Copper and Galvanized Iron Substrates. *Langmuir* **2008**, *24*, 10895−10900.
(9) Ma, Z.; Yu, H.; Jiang, W. Bump-Surface Multicompartment Micelles from a Linear ABC Triblock Copolymer: A Combination Study by Experiment and Computer Simulation. *J. Phys. Chem. B* **2009**, *113*, 3333−3338.
(10) Li, W.; Shi, A.-C. Theory of Hierarchical Lamellar Structures from $A(BC)_nBA$ Multiblock Copolymers. *Macromolecules* **2009**, *42*, 811−819.
(11) Klymko, T.; Markov, V.; Subbotin, A.; ten Brinke, G. Lamellar-in-Lamellar Self-Assembled C-*b*-$(B$-*b*-$A)_m$-*b*-B-*b*-C Multiblock Copolymers: Alexander-de Gennes Approach and Dissipative Particle Dynamics Simulations. *Soft Matter* **2009**, *5*, 98−103.
(12) Masuda, J.; Takano, A.; Suzuki, J.; Nagata, Y.; Noro, A.; Hayashida, K.; Matsushita, Y. Composition-Dependent Morphological Transition of Hierarchically-Ordered Structures Formed by Multiblock Terpolymers. *Macromolecules* **2007**, *40*, 4023−4027.
(13) Wang, L.; Zhang, L.; Lin, J. Hierarchically Ordered Microstructures Self-Assembled from $A(BC)_n$ Multiblock Copolymers. *Macromolecules* **2010**, *43*, 1602−1609.
(14) Morkved, T. L.; Lu, M.; Urbas, A. M.; Ehrichs, E. E.; Jaeger, H. M.; Mansky, P.; Russell, T. P. Local Control of Microdomain Orientation in Diblock Copolymer Thin Films with Electric Fields. *Science* **1996**, *273*, 931−933.
(15) Thurn-Albrecht, T.; Schotter, J.; Kastle, C. A.; Emley, N.; Shibauchi, T.; Krusin-Elbaum, L.; Guarini, K.; Black, C. T.; Tuominen, M. T.; Russell, T. P. Ultrahigh-Density Nanowire Arrays Grown in Self-Assembled Diblock Copolymer Templates. *Science* **2000**, *290*, 2126−2129.
(16) Kellogg, G. J.; Walton, D. G.; Mayes, A. M.; Lambooy, P.; Russell, T. P.; Gallagher, P. D.; Satija, S. K. Observed Surface Energy Effects in Confined Diblock Copolymers. *Phys. Rev. Lett.* **1996**, *76*, 2503−2506.
(17) Huang, E.; Rockford, L.; Russell, T. P.; Hawker, C. J. Nanodomain Control in Copolymer Thin Films. *Nature* **1998**, *395*, 757−758.
(18) Shin, K.; Xiang, H. Q.; Moon, S. I.; Kim, T.; McCarthy, T. J.; Russell, T. P. Curving and Frustrating Flatland. *Science* **2004**, *306*, 76−76.
(19) Yu, B.; Sun, P.; Chen, T.; Jin, Q.; Ding, D.; Li, B.; Shi, A.-C. Confinement-Induced Novel Morphologies of Block Copolymers. *Phys. Rev. Lett.* **2006**, *96*, 138306-1−138306-4.
(20) Turner, M. S. Equilibrium Properties of a Diblock Copolymer Lamellar Phase Confined between Flat Plates. *Phys. Rev. Lett.* **1992**, *69*, 1788−1791.
(21) Lambooy, P.; Russell, T. P.; Kellogg, G. J.; Mayes, A. M.; Gallagher, P. D.; Satija, S. K. Observed Frustration in Confined Block Copolymers. *Phys. Rev. Lett.* **1994**, *72*, 2899−2902.
(22) Knoll, A.; Horvat, A.; Lyakhova, K. S.; Krausch, G.; Sevink, G. J. A.; Zvelindovsky, A. V.; Magerle, R. Phase Behavior in Thin Films of Cylinder-Forming Block Copolymers. *Phys. Rev. Lett.* **2002**, *89*, 035501-1−035501-4.
(23) Segalman, R. A.; Yokoyama, H.; Kramer, E. J. Graphoepitaxy of Spherical Domain Block Copolymer Films. *Adv. Mater.* **2001**, *13*, 1152−1155.
(24) Kim, S. O.; Solak, H. H.; Stoykovich, M. P.; Ferrier, N. J.; de Pablo, J. J.; Nealey, P. F. Epitaxial Self-Assembly of Block Copolymers on Lithographically Defined Nanopatterned Substrates. *Nature* **2003**, *424*, 411−414.
(25) Park, S.; Lee, D. H.; Xu, J.; Kim, B.; Hong, S. W.; Jeong, U.; Xu, T.; Russell, T. P. Macroscopic 10-Terabit-per-Square-Inch Arrays from Block Copolymers with Lateral Order. *Science* **2009**, *323*, 1030−1033.
(26) Hamley, I. W. Nanostructure Fabrication Using Block Copolymers. *Nanotechnology* **2003**, *14*, R39.
(27) Park, C.; Yoon, J.; Thomas, E. L. Enabling Nanotechnology with Self-Assembled Block Copolymer Patterns. *Polymer* **2003**, *44*, 6725−6760.
(28) Koneripalli, N.; Singh, N.; Levicky, R.; Bates, F. S.; Gallagher, P. D.; Satija, S. K. Confined Block Copolymer Thin Films. *Macromolecules* **1995**, *28*, 2897−2904.
(29) Koneripalli, N.; Levicky, R.; Bates, F. S.; Ankner, J.; Kaiser, H.; Satija, S. K. Confinement-Induced Morphological Changes in Diblock Copolymer Films. *Langmuir* **1996**, *12*, 6681−6690.
(30) Huang, E.; Russell, T. P.; Harrison, C.; Chaikin, P. M.; Register, R. A.; Hawker, C. J.; Mays, J. Using Surface Active Random Copolymers To Control the Domain Orientation in Diblock Copolymer Thin Films. *Macromolecules* **1998**, *31*, 7641−7650.
(31) Russell, T. P.; Menelle, A.; Anastasiadis, S. H.; Satija, S. K.; Majkrzak, C. F. Unconventional Morphologies of Symmetric, Diblock Copolymers Due to Film Thickness Constraints. *Macromolecules* **1991**, *24*, 6263−6269.
(32) Morkved, T. L.; Jaeger, H. M. Thickness-Induced Morphology Changes in Lamellar Diblock Copolymer Ultrathin Films. *Europhys. Lett.* **1997**, *40*, 643−648.
(33) Matsen, M. W. Thin Films of Block Copolymer. *J. Chem. Phys.* **1997**, *106*, 7781−7791.
(34) Ludwigs, S.; Krausch, G.; Magerle, R.; Zvelindovsky, A. V.; Sevink, G. J. A. Phase Behavior of ABC Triblock Terpolymers in Thin Films: Mesoscale Simulations. *Macromolecules* **2005**, *38*, 1859−1867.
(35) Lin, S.; Numasawa, N.; Nose, T.; Lin, J. Brownian Molecular Dynamics Simulation on Self-Assembly Behavior of Rod-Coil Diblock Copolymers. *Macromolecules* **2007**, *40*, 1684−1692.
(36) Wang, R.; Wang, Z.-G. Theory of Side-Chain Liquid Crystal Polymers: Bulk Behavior and Chain Conformation. *Macromolecules* **2010**, *43*, 10096−10106.
(37) Zhang, L.; Lin, J.; Lin, S. Self-Assembly Behavior of Amphiphilic Block Copolymer/Nanoparticle Mixture in Dilute Solution Studied by

DOI: 10.1021/la503985u
Langmuir 2015, 31, 2533−2544

Self-Consistent-Field Theory/Density Functional Theory. *Macromolecules* **2007**, *40*, 5582−5592.
(38) Zhang, L.; Wang, L.; Lin, J. Harnessing Anisotropic Nanoposts to Enhance Long-Range Orientation Order of Directed Self-Assembly Nanostructures via Large Cell Simulations. *ACS Macro Lett.* **2014**, *3*, 712−716.
(39) Hoogerbrugge, P. J.; Koelman, J. M. V. A. Simulating Microscopic Hydrodynamic Phenomena with Dissipative Particle Dynamics. *Europhys. Lett.* **1992**, *19*, 155−160.
(40) Koelman, J. M. V. A.; Hoogerbrugge, P. J. Dynamic Simulations of Hard-Sphere Suspensions Under Steady Shear. *Europhys. Lett.* **1993**, *21*, 363−368.
(41) Jiang, T.; Wang, L.; Lin, S.; Lin, J.; Li, Y. Structural Evolution of Multicompartment Micelles Self-Assembled from Linear ABC Triblock Copolymer in Selective Solvents. *Langmuir* **2011**, *27*, 6440−6448.
(42) Feng, J.; Liu, H.; Hu, Y. Mesophase Separation of Diblock Copolymer Confined in a Cylindrical Tube Studied by Dissipative Particle Dynamics. *Macromol. Theory Simul.* **2006**, *15*, 674−685.
(43) Sheng, Y. J.; Nung, C. H.; Tsao, H. K. Morphologies of Star-Block Copolymers in Dilute Solutions. *J. Phys. Chem. B* **2006**, *110*, 21643−21650.
(44) Groot, R. D.; Warren, P. B. Dissipative Particle Dynamics: Bridging the Gap between Atomistic and Mesoscopic Simulation. *J. Chem. Phys.* **1997**, *107*, 4423−4435.
(45) Allen, M. P.; Tildesley, D. J. *Computer Simulation of Liquids*; Clarendon Press: Oxford, U.K., 1987.
(46) Espanol, P.; Warren, P. Statistical Mechanics of Dissipative Particle Dynamics. *Europhys. Lett.* **1995**, *30*, 191−196.
(47) Guo, H. X.; Kremer, K. Amphiphilic Lamellar Model Systems under Dilation and Compression: Molecular Dynamics Study. *J. Chem. Phys.* **2003**, *118*, 7714−7723.
(48) Guo, H. X. Shear-induced Parallel-to-Perpendicular Orientation Transition in the Amphiphilic Lamellar Phase: A Nonequibrium Molecular-Dynamics Simulation Study. *J. Chem. Phys.* **2006**, *124*, 054902-1−054902-11.
(49) Cai, C.; Wang, L.; Lin, J.; Zhang, X. Morphology Transformation of Hybrid Micelles Self-Assembled from Rod-Coil Block Copolymer and Nanoparticles. *Langmuir* **2012**, *28*, 4515−4524.
(50) Wang, L.; Lin, J.; Zhang, L. Hierarchically Ordered Microstructures Self-Assembled from Com-Coil Block Copolymers. *Langmuir* **2009**, *25*, 4735−4742.
(51) van Zoelen, W.; Asumaa, T.; Ruokolainen, J.; Ikkala, O.; ten Brinke, G. Phase Behavior of Solvent Vapor Annealed Thin Films of PS-*b*-P4VP(PDP) Supramolecules. *Macromolecules* **2008**, *41*, 3199−3208.
(52) Stoykovich, M. P.; Kang, H.; Daoulas, K. C.; Liu, G.; Liu, C.-C.; de Pablo, J. J.; Müller, M.; Nealey, P. F. Directed Self-Assembly of Block Copolymers for Nanolithography: Fabrication of Isolated Features and Essential Integrated Circuit Geometries. *ACS Nano* **2007**, *1*, 168−175.

DOI: 10.1021/la503985u
Langmuir 2015, 31, 2533−2544